11th World Congress on Structural and Multidisciplinary Optimisation
07th -12th, June 2015, Sydney Australia

Shape Optimization Method of Shell Structures Concerned with Material and Geometrical Nonlinearity

Shintaro Kosaka[1], **Masatoshi Shimoda**[2]

[1] Graduate school of engineering Toyota Technological Institute, Hisakata, Tenpaku-ku, Nagoya, Aichi, Japan, sd14409@toyota-ti.ac.jp
[2] Toyota Technological Institute, Hisakata, Tenpaku-ku, Nagoya, Aichi, Japan, shimoda@toyota-ti.ac.jp

1. Abstract

In this paper, we present a solution to a reaction force control problem of a shell structure based on the free-form optimization method for shells concerned with material nonlinearity and geometrical nonlinearity. The sum of squared error norms subjected to a specified force is minimized under a volume constraint. The shape optimum design problem is formulated as a distributed-parameter system under the assumptions that a shell is varied in the out-of-plane direction to the surface, whereas the thickness is not varied with respect to the shape change. The shape gradient function and the optimal conditions for this problem are theoretically derived using the material derivative method and the Lagrange multiplier method. The derived shape gradients are applied to the H^1 gradient method for shells, which was proposed one of the authors, to determine the optimal shape variation. The optimal shape of shell structures can be obtained without the shape parameterization, while maintaining the surface smoothness. The shape gradient function is calculated by a user sub-program which is developed using the result of non-linear FEM analysis based on a commercial solver. Several numerical examples are presented to verify the validity and practical utility of the proposed methodology and the developed system.

2. Keywords: FEM, Shape Optimization, Shell Structure, Material Nonlinear, Geometrical Nonlinear

3. Introduction

Shell structures have been widely utilized for automobile, train, airplane, architecture structure and so on. For instance, structures for energy absorption sometimes called crash box are attached to the end of an automobile or a train. Suspensions of automobiles are generally required to maximize the reaction force towards to an unexpected load. Moreover, structure dumpers are developed to absorb a seismic energy by the plastic deformation in the design of civil structures or buildings. Material nonlinearity and geometrical nonlinearity should be concerned in these design problem with large deformation and elasto-plasticity.

Some shape optimization methods concerning with material nonlinearity or geometrical nonlinearity have been published. Kaneko et al. [1] implement size optimization concerned with material non-linearity that is not path-dependent toward direct proportion load. And, Ryu et al. [2] showed sensibility analysis method for size optimization concerned with material non-linearity that is not path-dependent by the direct differentiation method. Thus, Ihara et al. [3] proposed a nonparametric design method for the compliance minimization problem concerned with material nonlinearity and the displacement control problem concerned with geometrical nonlinearity. Shintani et al. [4] proposed a solution method based on the H^1 gradient method for the mass minimization problem of 3D suspension parts subjected to the reaction force constraint.

In ours previous research, one of the authors proposed a shape optimization method for design of shell structures, and applied it to a linear stiffness problem and a linear frequency problem. In this work, we aim at developing a shape optimization method concerned with material nonlinearity and geometrical nonlinearity for controlling the reaction forces to equal to target values by applying the free-form optimization method for shells. We formulate the problem as a distributed parameter system, in which the squared error norm of the reaction forces to the target values is minimized under the volume constraint. The optimal shape variation is determined by the H^1 gradient method for shells.

In the following sections, domain variation for free-form design and the governing equation of the shell structure are described. Then, the formulation of the design problem and the derivation of the shape gradient function are presented. After introducing the free-form optimization method in detail, the validity and practical utility of this method are verified through several design examples at last.

4. Governing equation for a shell as a set of infinitesimal flat surfaces

As shown in Fig.1 (a) and (b) and Eqs.(1)-(3), consider that a shell having an initial bounded domain $\Omega \subset \mathbb{R}^3$ (boundary of $\partial\Omega$), mid-area A (boundary of ∂A) and side surface S undergoes domain variation in the out-of-plane direction to the surface so that its domain, mid-area and side-surface become Ω_s , A_S and S_S , respectively. The notation dA expresses a small area. The subscript s indicates the iteration history of domain variation. It is assumed that the plate thickness h keeps a constant under the domain variation.

$$\Omega=\left\{(x_1,x_2,x_3)\in\mathbb{R}^3 \mid (x_1,x_2)\in A\subset\mathbb{R}^2, x_3\in(-\frac{h}{2},\frac{h}{2})\right\},\quad \Omega=A\times(-\frac{h}{2},\frac{h}{2}),\quad S=\partial A\times(-\frac{h}{2},\frac{h}{2}) \tag{1}$$

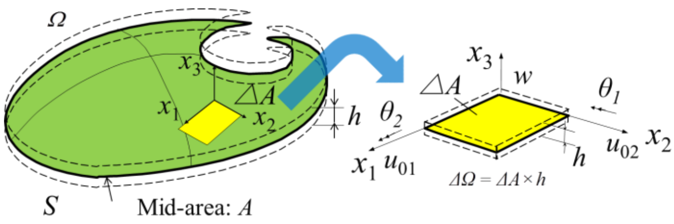

Figure 1: Shell as a set of infinitesimal flat surfaces.

The Mindlin-Reissner plate theory is used for concerning plate bending, whereas coupling of the membrane stiffness and bending stiffness is ignored. The displacement expressed by the local coordinates $\boldsymbol{u}=\{u_i\}_{i=1,2,3}$ are divided in the in-plane directions $\{u_\alpha\}_{\alpha=1,2}$ and the out-of-plane direction u_3, given as

$$u_\alpha(x_1,x_2,x_3)=u_{0\alpha}(x_1,x_2)-x_3\theta_\alpha(x_1,x_2) \tag{2}$$
$$u_3(x_1,x_2,x_3)=w(x_1,x_2) \tag{3}$$

where $\boldsymbol{u}_0=\{u_{0\alpha}\}_{\alpha=1,2}$, w and $\boldsymbol{\theta}=\{\theta_\alpha\}_{\alpha=1,2}$ express the in-plane displacement, out-of-plane displacement and rotational angle of the mid-area of the plate, respectively. The tensor subscript notation with respect to $\alpha=1,2$ uses Einstein's summation convention and a partial differential notation for the spatial coordinates $(\cdot)_{,i}=\partial(\cdot)/\partial x_i$.

Then, the weak form of the equilibrium equation for $(\boldsymbol{u}_0,w,\boldsymbol{\theta})\in U$ can be expressed as

$$a\left((\boldsymbol{u}_0,w,\boldsymbol{\theta}),(\bar{\boldsymbol{u}}_0,\bar{w},\bar{\boldsymbol{\theta}})\right)=l\left(\bar{\boldsymbol{u}}_0,\bar{w},\bar{\boldsymbol{\theta}}\right)-l_h\left(\bar{\boldsymbol{u}}_0,\bar{w},\bar{\boldsymbol{\theta}}\right),\quad \forall\left(\bar{\boldsymbol{u}}_0,\bar{w},\bar{\boldsymbol{\theta}}\right)\in U \tag{4}$$

where $(\bar{\bullet})$ expresses a variation. In addition, the bilinear symmetric form $a(\bullet,\bullet)$ and the linear form $l(\bullet)$ are defined as, respectively.

$$\begin{aligned}&a\left((\boldsymbol{u}_0,w,\boldsymbol{\theta}),(\bar{\boldsymbol{u}}_0,\bar{w},\bar{\boldsymbol{\theta}})\right)\\&=\int_\Omega\{S_{\alpha\beta}(u(\boldsymbol{u}_0,w,\boldsymbol{\theta}))\bar{E}_{\alpha\beta}(\bar{u}(\bar{\boldsymbol{u}}_0,\bar{w},\bar{\boldsymbol{\theta}}))+2S_{\alpha3}(u(\boldsymbol{u}_0,w,\boldsymbol{\theta}))\bar{E}_{\alpha3}(\bar{u}(\bar{\boldsymbol{u}}_0,\bar{w},\bar{\boldsymbol{\theta}}))\}dx\\&=\int_\Omega[C_{\alpha\beta\gamma\delta}(\boldsymbol{E})\{u_{\gamma,\delta}+\frac{1}{2}u_{l,\gamma}u_{l,\delta}\}\{\bar{u}_{\alpha,\beta}+\frac{1}{2}\bar{u}_{l,\alpha}\bar{u}_{l,\beta}\}+C^S_{\alpha\beta}(\boldsymbol{E})\{w_{,\beta}-\theta_\beta-u_{\eta,\beta}\theta_\eta\}\{\bar{w}_{,\alpha}-\bar{\theta}_\alpha-\bar{u}_{\eta,\alpha}\bar{\theta}_\eta\}]dx\end{aligned} \tag{5}$$

$$l\left((\bar{\boldsymbol{u}}_0,\bar{w},\bar{\boldsymbol{\theta}})\right)=-\int_A Fw\,dA+\int_{Sg}(N_\alpha u_{0\alpha}+M_\alpha\theta_\alpha-Qw)dS \tag{6}$$

$$\begin{aligned}l_h\left((\bar{\boldsymbol{u}}_0,\bar{w},\bar{\boldsymbol{\theta}})\right)=&\int_\Omega[C_{\alpha\beta\gamma\delta}(\boldsymbol{E})\{h_{\gamma,\delta}+\frac{1}{2}(h_{\eta,\gamma}u_{\eta,\delta}+u_{\eta,\gamma}h_{\eta,\delta}+h_{\eta,\gamma}h_{\eta,\delta})\}\{\bar{u}_{\alpha,\beta}+\frac{1}{2}\bar{u}_{l,\alpha}\bar{u}_{l,\beta}\}\\&+C^S_{\alpha\beta}(\boldsymbol{E})\{w^h_{,\beta}-\theta^h_\beta-h_{\eta,\beta}\theta_\eta-u_{\eta,\beta}\theta^h_\eta-h_{\eta,\beta}\theta^h_\eta\}\{\bar{w}_{,\alpha}-\bar{\theta}_\alpha-\bar{u}_{\eta,\alpha}\bar{\theta}_\eta\}]dx\end{aligned} \tag{7}$$

where S_{ij} and E_{ij} express the 2nd Piola-Kirchhoff stress and the Green-Lagrange strain tensor, respectively.
In order to assume that the enforced displacement is a monotonous increasing function, $\{C_{\alpha\beta\gamma\delta}(\boldsymbol{E})\}_{\alpha,\beta,\gamma,\delta=1,2}$ and $\{C^S_{\alpha\beta}(\boldsymbol{E})\}_{\alpha,\beta=1,2}$ express an elastic tensor including bending and membrane components and an elastic tensor with respect to the shear component, which are functions of strain tensor in the total strain theory.
$\boldsymbol{f}=\{f_\alpha\}_{\alpha=1,2}$, $\boldsymbol{m}=\{m_\alpha\}_{\alpha=1,2}$ and q express the in-plane load, the out-of-plane bending moment and the out-of-plane load, respectively. $\boldsymbol{N}=\{N_\alpha\}_{\alpha=1,2}$, $\boldsymbol{M}=\{M_\alpha\}_{\alpha=1,2}$ and Q express the in-plane load, the bending moment and the shear force, respectively.
The enforced displacement $\boldsymbol{h}=\{h_i\}_{i=1,2,3}$ is divided into components in the in-plane direction $\{h_\alpha\}_{\alpha=1,2}$ and in the out-of-plane direction h_3.

$$h_\alpha(x_1,x_2,x_3)=u^h_{0\alpha}(x_1,x_2)-x_3\theta^h_\alpha(x_1,x_2) \tag{8}$$
$$h_3(x_1,x_2,x_3)=w^h(x_1,x_2) \tag{9}$$

where $\boldsymbol{u}^h_0=\{u^h_{0\alpha}\}_{\alpha=1,2}$, w^h and $\theta=\{\theta^h_\alpha\}_{\alpha=1,2}$ express the displacement vector in the in-plane direction, the flexure and the rotational angles of the mid-area of the plate, respectively. The subscripts of the Greek letters are expressed as $\alpha,\beta,\gamma,\delta,\eta=1,2$.

5. Formulation of the reaction forces control problem
The reaction forces control problem under a volume and the state equation (Eq. (4)) constraints is formulated as a distributed-parameter system. The design variable to be determined is the design velocity field $\boldsymbol{V}$.
When the *NB* control points are considered to a shell, the weak form of the equilibrium on *p*th control point can be expressed as Eq. (13) to control the reaction forces. $c^{(p)}$ indicates the weighting coefficient for the *p*th control point in Fig.2.

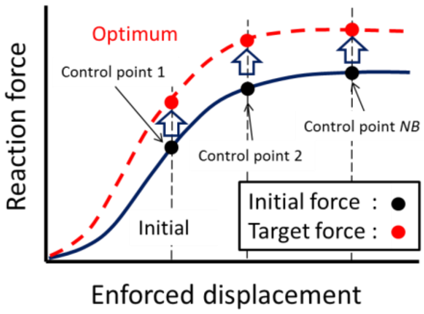

Figure 2: The reaction forces control problem

$$\text{Given} \quad A,\hat{M}, \tag{10}$$
$$\text{Find} \quad V, \tag{11}$$
$$\text{that minimize} \quad \sum_{p=1}^{NB} c^{(p)}\left[I(\boldsymbol{r}\cdot\boldsymbol{T}^{(p)})-\hat{T}^{(p)}\right]^2, \tag{12}$$
$$\text{subject to} \quad a\left(\left(\boldsymbol{u}_0{}^{(p)},w^{(p)},\boldsymbol{\theta}^{(p)}\right),\left(\bar{\boldsymbol{u}}_0{}^{(p)},\bar{w}^{(p)},\bar{\boldsymbol{\theta}}^{(p)}\right)\right)=l\left(\bar{\boldsymbol{u}}_0{}^{(p)},\bar{w}^{(p)},\bar{\boldsymbol{\theta}}^{(p)}\right)-l_h\left(\bar{\boldsymbol{u}}_0{}^{(p)},\bar{w}^{(p)},\bar{\boldsymbol{\theta}}^{(p)}\right),$$
$$\forall(\bar{\boldsymbol{u}}_0{}^{(p)},\bar{w}^{(p)},\bar{\boldsymbol{\theta}}^{(p)})\in U,(\boldsymbol{u}_0{}^{(p)},w^{(p)},\boldsymbol{\theta}^{(p)})\in U,\ p=1,\cdots,NB \tag{13}$$
$$M(=\int_A h\,dA)\le\hat{M} \tag{14}$$

where, $I(\boldsymbol{r}\cdot\boldsymbol{T}^{(p)})$ can be expressed as

$$I(\boldsymbol{r}\cdot\boldsymbol{T}^{(p)})=\int_{A_D} r_i T_i^{(p)}dA=\int_{A_D} r_i S_{ij}^{(p)} n_j^{(p)}dA \tag{15}$$

where $\boldsymbol{r}=\{r_i\}_{i=1,2,3}$ expresses the unit vector of the enforced displacement direction. $\boldsymbol{T}^{(p)}=\{T_i\}^{(p)}_{i=1,2,3}=S^{(p)}_{ij}n^{(p)}_j$, $n^{(p)}_i$ and $\hat{T}^{(p)}$ express the stress vector, the normal vector to the surface and the target force, respectively. M and $\hat{M}$ denote the volume and its constraint value, respectively. Letting $(\bar{\boldsymbol{u}}_0,\bar{w},\bar{\boldsymbol{\theta}})$ and Λ denote the Lagrange multiplier for the state equation and the volume constraint, respectively, the Lagrange functional L associated with this problem can be expressed as

$$
\begin{aligned}
L=&\sum_{p=1}^{NB}c^{(p)}\left[I(\boldsymbol{r}\cdot\boldsymbol{T}^{(p)})-\hat{T}\right]^2\\
&+\sum_{p=1}^{NB}\left\{l\left(\bar{\boldsymbol{u}}_0{}^{(p)},\bar{w}^{(p)},\bar{\boldsymbol{\theta}}^{(p)}\right)-l_h\left(\bar{\boldsymbol{u}}_0{}^{(p)},\bar{w}^{(p)},\bar{\boldsymbol{\theta}}^{(p)}\right)-a\left(\left(\boldsymbol{u}_0{}^{(p)},w^{(p)},\boldsymbol{\theta}^{(p)}\right),\left(\bar{\boldsymbol{u}}_0{}^{(p)},\bar{w}^{(p)},\bar{\boldsymbol{\theta}}^{(p)}\right)\right)\right\}\\
&+\Lambda\left(M-\hat{M}\right)
\end{aligned}
\tag{16}
$$

For the sake of simplicity here, it is assumed that on the sub-boundaries, the non-zero boundary forces ***N***, ***Q*** and ***M*** and the surface forces ***f***, ***m*** and q, do not vary with regard to the space (i.e., $\boldsymbol{f}'=\boldsymbol{m}'=q'=0$). Then, using the design velocity field ***V***, the derivative $\dot{L}$ of the domain variation of the Lagrange functional L can be expressed as

$$
\begin{aligned}
\dot{L}=&\sum_{p=1}^{NB}\left\{c^{(p)}2\left[I(\boldsymbol{r}\cdot\boldsymbol{T}^{(p)})-\hat{T}^{(p)}\right]I(\boldsymbol{r}\cdot\boldsymbol{T}'^{(p)})-a\left(\left(\boldsymbol{u}_0{}'^{(p)},w'^{(p)},\boldsymbol{\theta}'^{(p)}\right),\left(\bar{\boldsymbol{u}}_0{}^{(p)},\bar{w}^{(p)},\bar{\boldsymbol{\theta}}^{(p)}\right)\right)\right\}\\
&+\sum_{p=1}^{NB}\left\{l\left(\bar{\boldsymbol{u}}_0{}'^{(p)},\bar{w}'^{(p)},\bar{\boldsymbol{\theta}}'^{(p)}\right)-a\left(\left(\boldsymbol{u}_0{}^{(p)},w^{(p)},\boldsymbol{\theta}^{(p)}\right),\left(\bar{\boldsymbol{u}}_0{}'^{(p)},\bar{w}'^{(p)},\bar{\boldsymbol{\theta}}'^{(p)}\right)\right)-l_h\left(\bar{\boldsymbol{u}}_0{}'^{(p)},\bar{w}'^{(p)},\bar{\boldsymbol{\theta}}'^{(p)}\right)\right\}\\
&+\dot{\Lambda}\left(M-\hat{M}\right)+\left\langle G\boldsymbol{n},\boldsymbol{V}\right\rangle,
\end{aligned}
\tag{17}
$$

where $\left\langle G\boldsymbol{n},\boldsymbol{V}\right\rangle=\int_A G\boldsymbol{n}\cdot\boldsymbol{V}dA=\int_A GV_n dA$.

$$
\begin{aligned}
G=&\sum_{p=1}^{NB}c^{(p)}(C^B_{\alpha\beta\gamma\delta}(\boldsymbol{E}^{(p)})\\
&\times[(u_{0\gamma,\delta}{}^{(p)}-\frac{h}{2}\theta_{\gamma,\delta}{}^{(p)})+\frac{1}{2}\{(u_{0\eta,\gamma}{}^{(p)}-\frac{h}{2}\theta_{\eta,\gamma}{}^{(p)})(u_{0\eta,\delta}{}^{(p)}-\frac{h}{2}\theta_{\eta,\delta}{}^{(p)})+w_{,\gamma}{}^{(p)}w_{,\delta}{}^{(p)}\}]\\
&\times[(\bar{u}_{0\alpha,\beta}{}^{(p)}-\frac{h}{2}\bar{\theta}_{\alpha,\beta}{}^{(p)})+\frac{1}{2}\{(\bar{u}_{0\eta,\alpha}{}^{(p)}-\frac{h}{2}\bar{\theta}_{\eta,\alpha}{}^{(p)})(\bar{u}_{0\eta,\beta}{}^{(p)}-\frac{h}{2}\bar{\theta}_{\eta,\beta}{}^{(p)})+\bar{w}_{,\alpha}{}^{(p)}\bar{w}_{,\beta}{}^{(p)}\}]\\
&-C^B_{\alpha\beta\gamma\delta}(\boldsymbol{E}^{(p)})[(u_{0\gamma,\delta}{}^{(p)}+\frac{h}{2}\theta_{\gamma,\delta}{}^{(p)})+\frac{1}{2}\{(u_{0\eta,\gamma}{}^{(p)}+\frac{h}{2}\theta_{\eta,\gamma}{}^{(p)})(u_{0\eta,\delta}{}^{(p)}+\frac{h}{2}\theta_{\eta,\delta}{}^{(p)})+w_{,\gamma}{}^{(p)}w_{,\delta}{}^{(p)}\}]\\
&\times[(\bar{u}_{0\alpha,\beta}{}^{(p)}+\frac{h}{2}\bar{\theta}_{\alpha,\beta}{}^{(p)})+\frac{1}{2}\{(\bar{u}_{0\eta,\alpha}{}^{(p)}-\frac{h}{2}\bar{\theta}_{\eta,\alpha}{}^{(p)})(\bar{u}_{0\eta,\beta}{}^{(p)}-\frac{h}{2}\bar{\theta}_{\eta,\beta}{}^{(p)})+\bar{w}_{,\alpha}{}^{(p)}\bar{w}_{,\beta}{}^{(p)}\}]\\
&-F^{(p)}\left(w_{,i}{}^{(p)}+\bar{w}_{,i}{}^{(p)}\right)n_i+\left\{-F^{(p)}\left(w^{(p)}+\bar{w}^{(p)}\right)+\Lambda h\right\}H)
\end{aligned}
\tag{18}
$$

where $\boldsymbol{V}_n=V_in_i$ and $(\cdot)'$ expresses a shape derivative. H denotes twice the mean curvature of the mid-area. C_Θ is the suitably smooth function space that satisfies the constraints of the domain variation. The notations $\boldsymbol{n}^{top}$ and $\boldsymbol{n}^{btm}$ denote unit outward normal vectors at the top surface and the bottom surface, respectively, and a unit normal vector at the mid-area $\boldsymbol{n}^{mid}(\equiv\boldsymbol{n})=\boldsymbol{n}^{top}=-\boldsymbol{n}^{btm}$ is assumed by Shimoda et al. [5].
The optimality conditions of the Lagrange functional L with respect to the state variables $(\boldsymbol{u}_0,w,\boldsymbol{\theta})$, the adjoint variables $(\bar{\boldsymbol{u}}_0,\bar{w},\bar{\boldsymbol{\theta}})$ and Λ are expressed as

$$a\left(\left(\boldsymbol{u}_0^{(p)}, w^{(p)}, \boldsymbol{\theta}^{(p)}\right), \left(\bar{\boldsymbol{u}}_0'^{(p)}, \bar{w}'^{(p)}, \bar{\boldsymbol{\theta}}'^{(p)}\right)\right) = l\left(\bar{\boldsymbol{u}}_0'^{(p)}, \bar{w}'^{(p)}, \bar{\boldsymbol{\theta}}'^{(p)}\right) - l_h\left(\bar{\boldsymbol{u}}_0'^{(p)}, \bar{w}'^{(p)}, \bar{\boldsymbol{\theta}}'^{(p)}\right),$$
$$\left(\boldsymbol{u}_0^{(p)}, w^{(p)}, \boldsymbol{\theta}^{(p)}\right) \in U, \quad \forall\left(\bar{\boldsymbol{u}}_0'^{(p)}, \bar{w}'^{(p)}, \bar{\boldsymbol{\theta}}'^{(p)}\right) \in U, \quad p = 1, \cdots, NB \tag{19}$$

$$a\left(\left(\boldsymbol{u}_0'^{(p)}, w'^{(p)}, \boldsymbol{\theta}'^{(p)}\right), \left(\bar{\boldsymbol{u}}_0^{(p)}, \bar{w}^{(p)}, \bar{\boldsymbol{\theta}}^{(p)}\right)\right) = c^{(p)} 2\left[I(\boldsymbol{r}\cdot\boldsymbol{T}^{(p)}) - \hat{T}^{(p)}\right] I(\boldsymbol{r}\cdot\boldsymbol{T}'^{(p)}),$$
$$\left(\bar{\boldsymbol{u}}_0^{(p)}, \bar{w}^{(p)}, \bar{\boldsymbol{\theta}}^{(p)}\right) \in U, \quad \forall\left(\boldsymbol{u}_0'^{(p)}, w'^{(p)}, \boldsymbol{\theta}'^{(p)}\right) \in U, \quad p = 1, \cdots, NB \tag{20}$$

$$\dot{\Lambda}\left(M - \hat{M}\right) = 0, \quad \dot{\Lambda} \geq 0, \; M - \hat{M} \leq 0. \tag{21}$$

where Eqs. (19) and (20) express the state equation for $(\boldsymbol{u}_0, w, \boldsymbol{\theta})$ and the adjoint equation for $(\bar{\boldsymbol{u}}_0, \bar{w}, \bar{\boldsymbol{\theta}})$, respectively. Eq. (21) denotes the governing equations for the volume constraint.

Substituting $(\boldsymbol{u}_0, w, \boldsymbol{\theta})$, $(\bar{\boldsymbol{u}}_0, \bar{w}, \bar{\boldsymbol{\theta}})$ and Λ determined by these equations into Eq. (17), the material derivative $\dot{L}$ can be expressed as

$$\dot{L} = \langle G\boldsymbol{n}, \boldsymbol{V} \rangle \equiv \int_A G_i V_i \, d\Gamma \tag{22}$$

where coefficient function G_i expresses the shape gradient function, which is used in H^1 gradient method for shells.

6. H^1 gradient method for shells

The original traction method was proposed by Azegami in 1994 and developed for free-form shell optimization by Shimoda et al. [5]. It is a node-based shape optimization method that treats all nodes as design variables and does not require any design variable parameterization. The shape gradient function is not used directly while replaced by a distributed force to vary the shape. The governing equation is expressed by Eq. (23). α is introduced to control influence range of the shape gradient function.

$$a((\boldsymbol{V}_{0\alpha}, V_3, \boldsymbol{\theta}), (\bar{\boldsymbol{u}}_0, \bar{w}, \bar{\boldsymbol{\theta}})) + \alpha\left\langle (\boldsymbol{V}\cdot\boldsymbol{n})\boldsymbol{n}, (\bar{\boldsymbol{u}}_0, \bar{w}, \bar{\boldsymbol{\theta}}) \right\rangle = -\left\langle G\boldsymbol{n}, (\bar{\boldsymbol{u}}_0, \bar{w}, \bar{\boldsymbol{\theta}}) \right\rangle$$
$$(\boldsymbol{V}_{0\alpha}, V_3, \boldsymbol{\theta}) \in C_\Theta, \quad \forall(\bar{\boldsymbol{u}}_0, \bar{w}, \bar{\boldsymbol{\theta}}) \in C_\Theta \tag{23}$$

7. Result of numerical analysis

FE model consists of constant strain triangle elements. Initial barrel-shaped model is shown in Fig.3. The enforced displacement by 1mm is applied at the right edge in the positive X direction and the left edge is clamped in the state and adjoint analyses. The objective is to control the reaction force to 5000N at the enforced displacement 1mm. And, the volume constraint is set as 1.01 times of initial shape. Both edges of the barrel-shaped model are clamped in the velocity analysis.

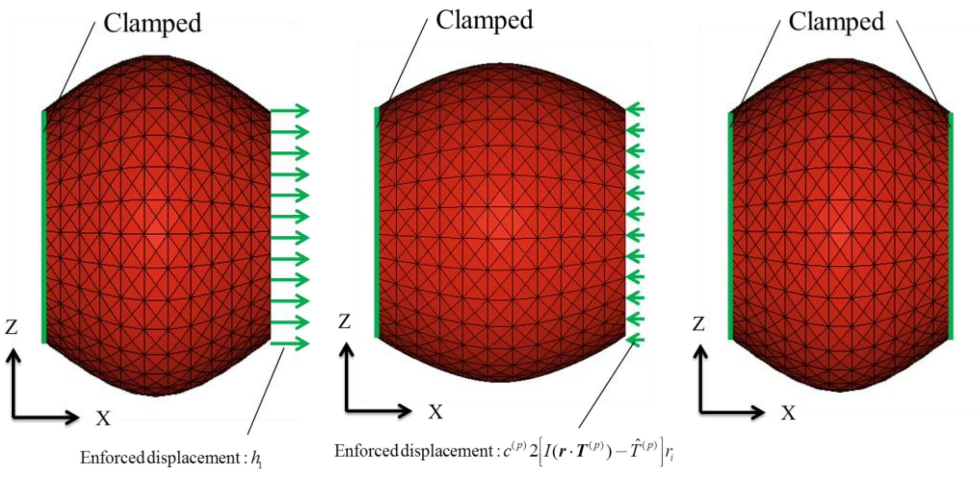

(a) State analysis (b) Adjoint analysis (c) Velocity analysis

Figure 3: Boundary conditions

Fig.4 shows the iteration histories of objective and volume (a), and reaction force (b). It is clear that the reaction force is equal to 5000N at the enforced displacement 1mm. Fig.5 (a) shows the optimized shape at the 100th iteration and (b) shows the reaction force-enforced displacement curves. It is confirmed that the reaction force changes from 6481N to 5000N at the enforced displacement 1mm. Curvature of the middle part of barrel becomes bigger that owns lower stiffness, at which are valid results.

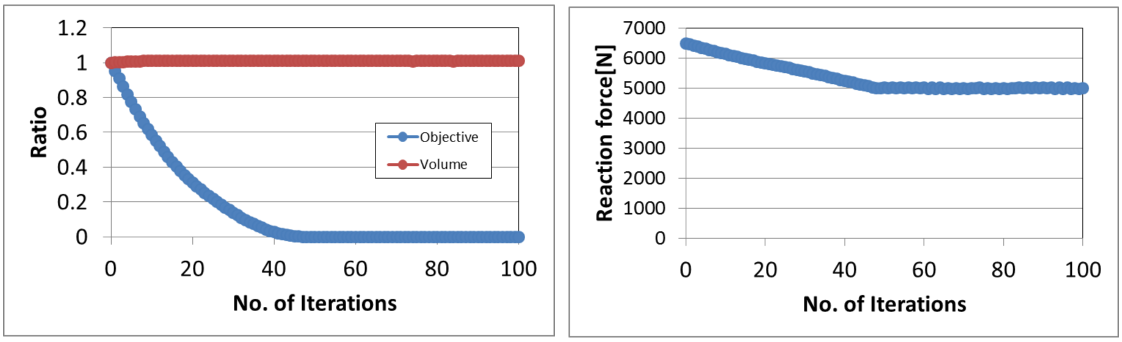

(a)Objective and volume (b)Reaction force

Figure 4: Iteration histories

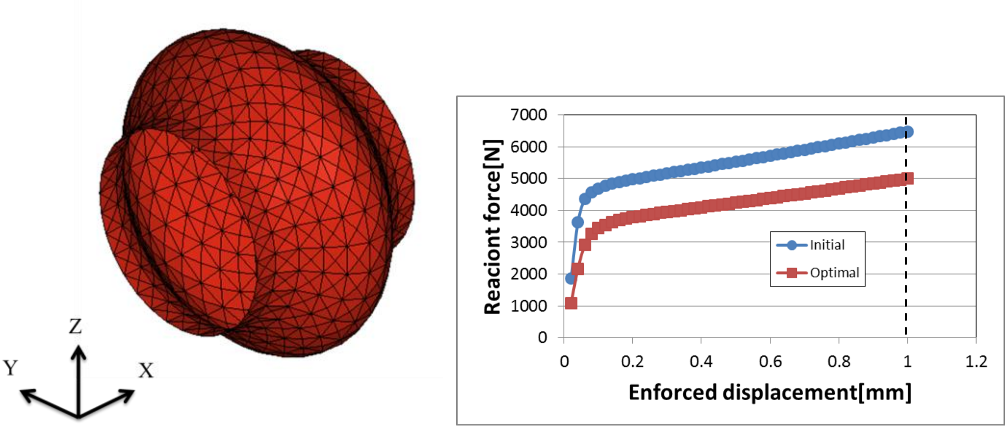

(a)Optimal shape (b)Reaction force-displacement curves

Figure 5: Optimization results

8. Conclusion

We presented a solution to a reaction force control problem of a shell structure based on the free-form optimization method for shells concerned with material nonlinearity and geometrical nonlinearity. With this method, the smooth out-of-plane domain variations for controlling the reaction forces to target values can be obtained. The results of a barrel-shaped model showed that the smooth optimal free-form shape and stable convergence histories were obtained.

With this method, it is easy to obtain the smooth optimal free-form shapes of shell structures without any shape design parameterization, and to control the reaction forces to target values.

9. References

[1] I. Kaneko and G. Maier, Optimum design of plastic structures under displacement constraint, *Computer methods in applied mechanics and engineering*, 27, 369-391, 1981.

[2] Y.S. Ryu, M. Hariman, C.C. Wu and J.S. Arora, Structural design sensitivity analysis of nonlinear response, *Computers & Structres*, 21, 245-255, 1985.

[3] H. Ihara, H. Azegami, M. Shimoda and K. Watanabe, Solution to Shape Optimization Problem Considering Material Nonlinearity, *Transactions of the JSME, Series A*, 66(646), 1111-1118, 2000. (in Japanese)

[4] K. Shintani, T. Nagatani, S. Ito and H. Azegami, Examination of Shape Optimization for the Nonlinear Buckling Phenomenon of Suspension Parts, *Transactions of the JSME, Series A*, 77(780), 1187-1198, 2011. (in Japanese)

[5] M. Shimoda, Free-Form Optimization Method for Shell Structures, *Transactions of the JSME, Series A*, 79(797), 60-73, 2013. (in Japanese)